JMEPEG (2010) 19:1–6
DOI: 10.1007/s11665-009-9411-0

©ASM International
1059-9495/$19.00

Research on the Friction and Wear Behavior at Elevated Temperature of Plasma-Sprayed Nanostructured WC-Co Coatings

Hui Chen, Guoqing Gou, Mingjing Tu, and Yan Liu

(Submitted April 6, 2008; in revised form February 19, 2009)

Nanostructured and ultra-fine WC-Co coatings were prepared by plasma spray. The friction and wear behavior at elevated temperature and failure mechanism were investigated. The results indicated that the sliding wear resistance of nanostructured coating is better than that of ultra-fine coating at high temperature. The wear mechanism is different between ultra-fine coating and nanostructured coating. Brittle fracture and adhesive wear dominate in ultra-fine coating followed with abrasive wear. Toughness fracture and abrasive wear dominate in nanostructured coating followed with adhesive wear.

Keywords nanostructured coatings, wear at elevated temperature, WC-Co

1. Introduction

Tungsten carbide has high hardness but low toughness, which restricts its application (Ref 1). The grain size of WC largely determines the mechanical properties of this cemented carbide. With the development of nano-technology, the preparation methods and technology of nano-WC powder become mature. When the grain size is reduced to nano-size range, not only the strength, hardness, and wear resistance can be significantly enhanced, but also the toughness can be improved (Ref 2-4). Therefore, using nano-WC powder as raw material makes it possible to prepare cemented carbide surface with high hardness and toughness.

Research indicated that the hardness and strength of WC-Co materials increase with decreasing WC grain size. The hardness, toughness, and resistance to abrasive wear of nanostructured WC-Co ceramic materials are higher than those of conventional WC-Co materials, which make it suitable for wider applications (Ref 5-9). In the spraying process, spraying process parameters and spraying equipment are important to maintain nanocrystallinity not to grow and obtain nanostructured coatings.

Yang et al. (Ref 10) researched the sliding wear behavior of HVOF-sprayed WC-12%Co coatings at elevated temperatures. Research indicated that the specific wear rate of the coatings increased with increasing WC grain size at a given testing temperature, and it decreased with increasing temperature for a given WC grain size. The formation of dense and adherent tribofilms plays an important role in the low sliding wear rate of the coatings at elevated temperatures. Yang et al. (Ref 11) investigated the effect of WC grain size on the microstructure and sliding wear behavior of HVOF-sprayed WC-12% Co coatings. The results showed that the specific wear rate of the coatings increased with increasing WC grain size. Cobalt extrusion followed by WC removal, or WC fracture is the predominant material removal mechanisms of the WC-Co coatings instead of splat delamination and binder/WC interfacial fracture. Zhao et al. (Ref 12) did research on the friction and wear behavior of plasma-sprayed conventional and nanostructured WC-12% Co coatings on stainless steel. The research noted that the wear rate of the conventional and nanostructured WC-12% Co coatings increased with increasing temperature, which is contradictory to the results of Yang et al. (Ref 10). The worn surfaces of the conventional WC-12% Co coating at different sliding conditions showed more severe adhesion, micro-fracture, and peeling as compared to the nanostructured WC-12% Co coating, which well conformed to the corresponding wear resistance of the two types of coatings.

WC-Co coating has excellent high temperature properties. Earlier studies researched its application below 540 °C, and few studies researched the friction and wear failure mechanism of WC-Co coatings at temperature higher than 400 °C. In this study, we researched the friction and wear behavior of nanostructured WC-Co coatings at 600 °C by using advanced high-temperature friction and wear test machine and the formation of nanostructured coatings in the plasma-sprayed process. The present work provides an appropriate theoretical basis for the application of WC-Co coating at high temperature.

2. Experimental Procedure

Plasma spraying equipment (GP80A type) is used to spray WC-17% Co on carbon steel (Q235) substrates. Two

---

Hui Chen, Institute of Materials Science and Engineering, Southwest Jiaotong University, Chengdu 610031, China and Institute of Materials Science and Engineering, Sichuan University, Chengdu 610041, China; and **Guoqing Gou** and **Yan Liu**, Institute of Materials Science and Engineering, Southwest Jiaotong University, Chengdu 610031, China; and **Mingjing Tu**, Institute of Materials Science and Engineering, Sichuan University, Chengdu 610041, China. Contact e-mail: xnrpt@swjtu.edu.cn.

Table 1 Powder properties

Feedstock powder	Feedstock size, µm	WC grain size, nm
Ultrafine WC-Co	15-45	600
Nanostructured WC-Co	15-45	50-500

Table 2 Plasma spraying parameters (top coating)

Spraying material	Current, A	Voltage, V	Ar, L/min	H_2, L/min	Powder feed gas (Ar), L/h
Ultrafine WC-Co	600	60	50	4	440
Nanostructured WC-Co	500	60	50	4	400

commercially available WC-Co powders sprayed are presented in Table 1. The spraying parameters are listed in Table 2.

The morphologies of WC-Co feedstocks, coatings, and worn surfaces were analyzed using a JSM-5910LV Scanning Electron Microscope (SEM) equipped with an Energy Dispersion X-ray (EDX), and HITACHI S4800 Field Launch Scanning Electron Microscope (FESEM). X-ray diffraction (XRD) was conducted for the phase composition of feedstocks and coatings using Cu $K\alpha$ radiation at a potential of 40 kV and current of 30 mA. The scanning speed of 2θ was 2°/min during the measurement.

The dry sliding wear tests were performed using GCr15 as mating material. The wear tests were done at sliding speed of 200 r/min, a constant load of 400 N and an elevated temperature setting of 600 °C. Weight loss of the specimens was measured by using a balance with an accuracy of ±0.1 mg. Friction coefficient was recorded automatically on sliding wear tester. Schematic of the tester was shown in Fig. 1.

3. Results

Figure 2 shows the morphologies of the WC-Co feedstock powders. From Fig. 2(a) and (c), it is found that the size of ultra-fine powder is relatively even and the powder shape shows regularly spherical, both of which are beneficial for enhancing spraying quality. Figure 2(b) and (d) indicates that the powder size of the nano WC-Co feedstock powder varies widely from several micrometers to about dozens of micrometers and the shape of the powder deviates from spherical, which may influence the spraying technology and coating quality.

Figure 3(a) shows the SEM morphology of surface of ultra-fine WC-Co coating. It is noted that there exist massive WC particles which are un-melted and coated by Co binder. Figure 3(b) indicates that the surface of nanostructured coating is smooth and most of the carbide has been melted. The SEM morphology of cross section (Fig. 3c and d) shows that the layer structure was not obvious in the ultra-fine coating and nanostructured coating. Pores are more in the nanostructured coating, which indicates that the degree of oxidation and decarbonization is more severe.

Figure 4 shows the FESEM morphology of the nanostructured coatings. It is noted that the particles are fine and distribute uniformly in nanostrutured coating. There exist amorphous and nanocrystalline particles. Nanocrystalline particles distribute uniformly and densely.

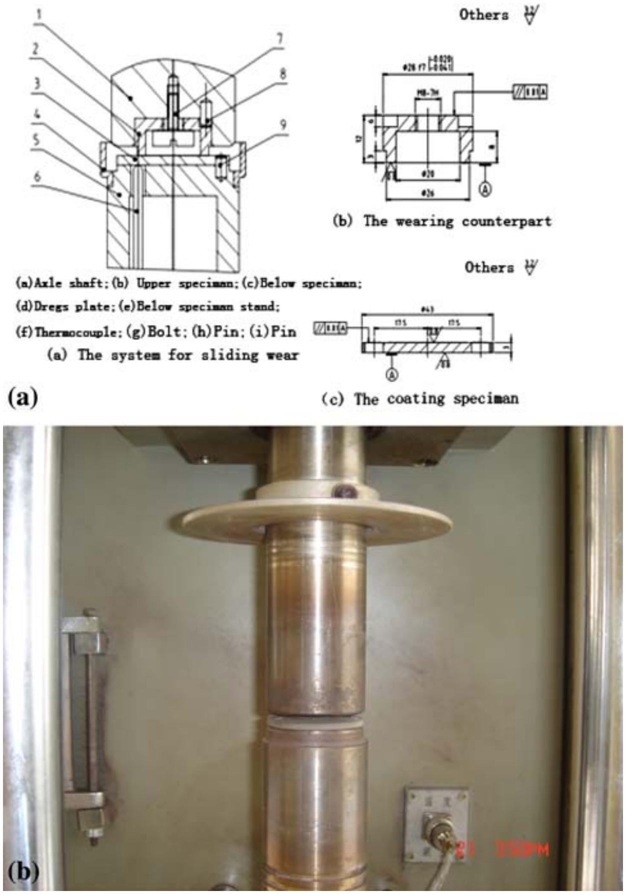

Fig. 1 System of wearing test (a) pin-disc wearing counterpart; (b) testing contact equipment

Figure 5 shows examples of XRD patterns of the powders and coatings. XRD spectra of ultra-fine coatings and nanostructured coatings are all composed of WC (hcp) and W_2C (hcp) phase. There is a little of Co_6W_6C phase existing in ultra-fine coatings. The ratios of the main peak height of W_2C at $2\theta = 39.7308°$ show that the strength in nanostructured coatings is much higher than that in ultra-fine coatings. The formation of W_2C is largely dependent on the degree of heating of the powders. Greater heating leads to more W_2C phase. The smaller the particle size, the higher the area-to-volume ratio, which leads to full melting, more decarbonization, and easier formation of W_2C. There was a broad peak between 42° and 44° corresponding to an amorphous phase in both coatings. The existence of amorphous phase has complicated influence on the strength, hardness, stiffness, toughness, and plasticity.

Figure 6 shows the variation of the friction coefficients for both the ultra-fine and nanostructured coatings sliding against GCr15 under un-lubricated conditions at a temperature of 600 °C. It can be seen that the friction coefficient for nanostructured WC-Co coating roughly recorded somewhat smaller fluctuations comparing with ultra-fine WC-Co coating. The friction coefficient of nanostructured coating is higher than that of ultra-fine coating at the beginning. With time, the friction coefficient of ultra-fine coating increases and becomes higher than that of nanostructured coating. The friction

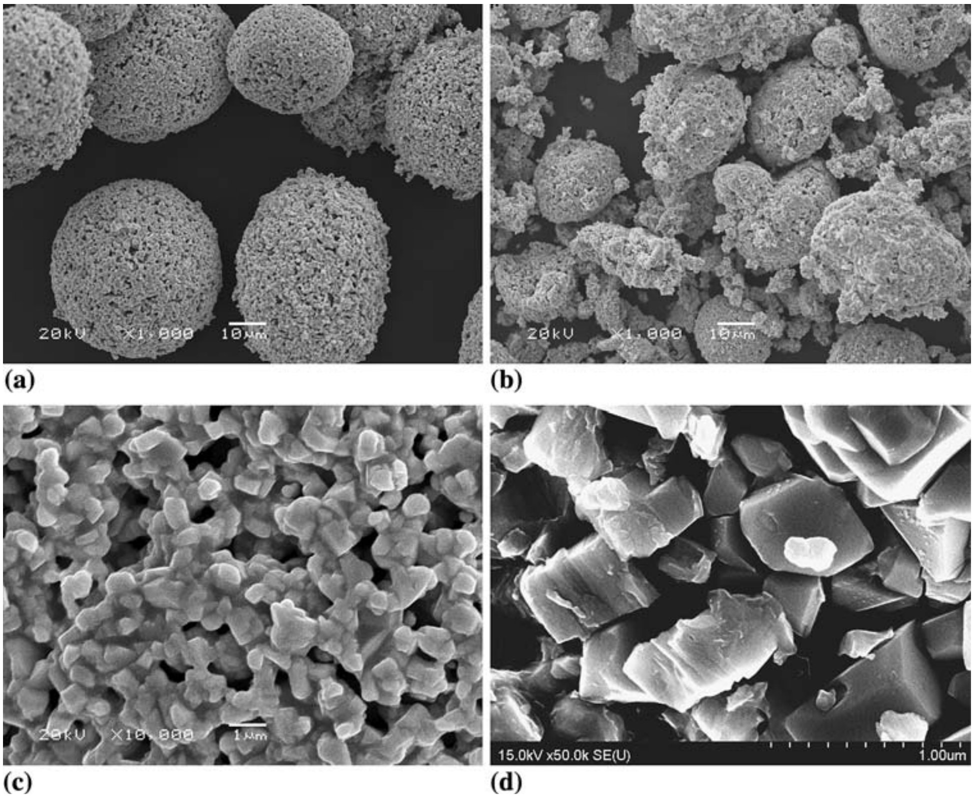

Fig. 2 Morphology of the powders: (a) ultra-fine powder; (b) nanostructured powder; (c) ultra-fine powder; and (d) nanostructured powder

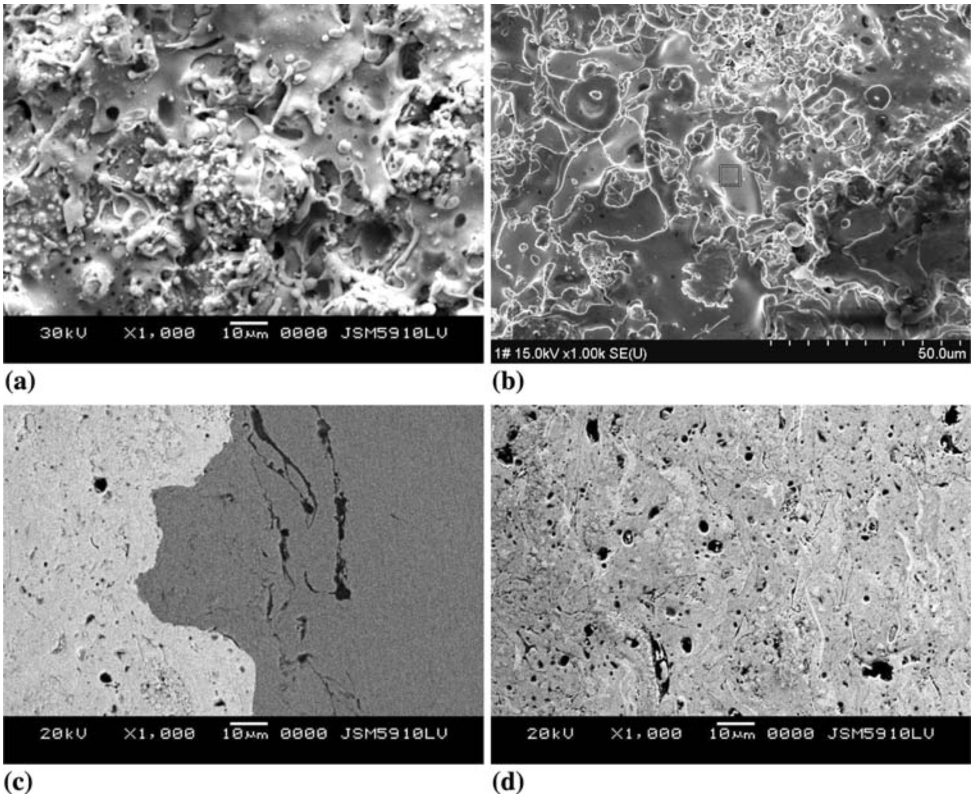

Fig. 3 SEM images of the coatings: (a) surface of ultra-fine WC-Co coating; (b) surface of nanostructured WC-Co coating; (c) cross-section of ultra-fine WC-Co coating; and (d) cross-section of nanostructured WC-Co coating

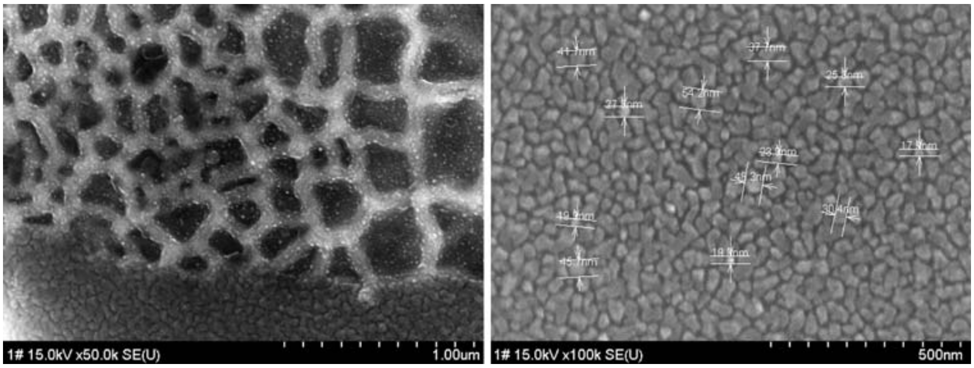

Fig. 4 FESEM images of the nanostructured coatings

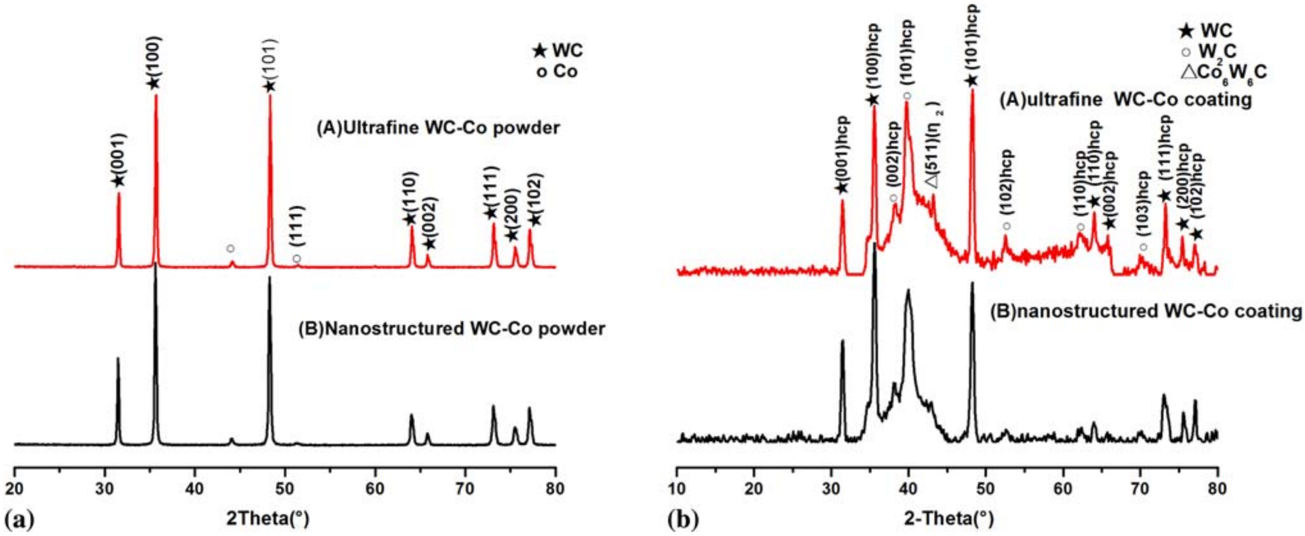

Fig. 5 Curves of coatings' phase composition: (a) powder and (b) coating

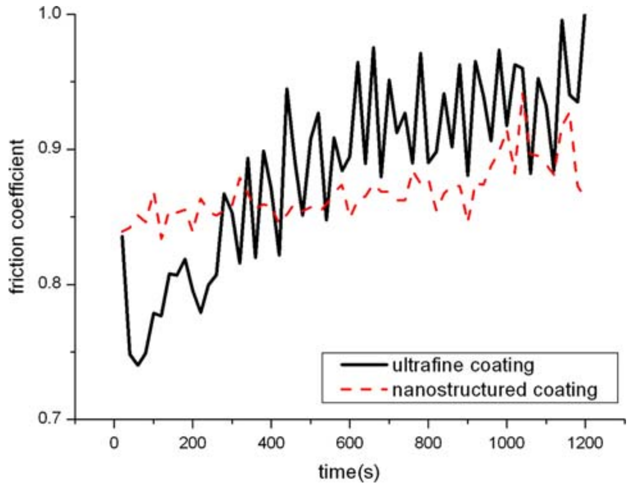

Fig. 6 Curves of the friction coefficient of the two type coatings

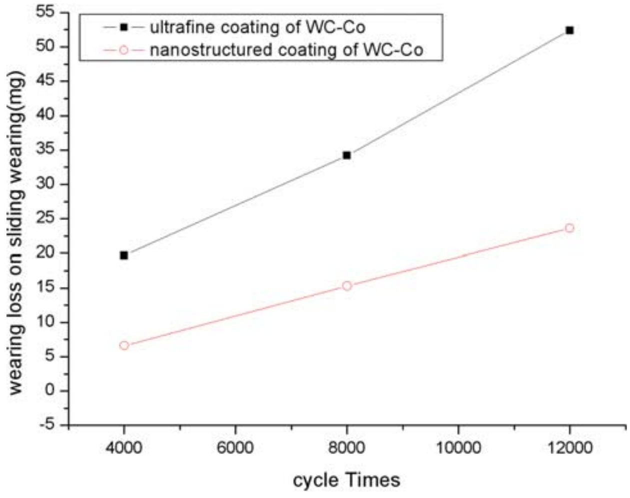

Fig. 7 Curves of the wear loss of the two type coatings

coefficient of both coatings increases with time. At first when slight wear is caused by plastic deformation, the friction coefficient is small. When abrasive wear happens, the effect of debris leads to increase in friction coefficient. When new surfaces form, the friction coefficient may decrease again.

Figure 7 shows the variation of the wear loss of the two type coatings. From Fig. 7, we can conclude that the wear loss is less in nanostructured coating, which indicates that at high temperature the wear resistance of nanostructured coating is better than that of ultra-fine coating.

4. Discussion

The reduction of WC grain size to the nanometer range will increase the hardness, porosity, wear resistance, and bonding strength. The improvement in such properties can be explained by the fact that as the carbide grain size decreases, the mean free path of Co matrix is reduced, which results in increased hardness according to the Hall-Patch (Ref 13) relationship and increased fracture toughness due to a greater amount of plastic deformation with cracking. These results reduce the indentation depth caused by the abrasive and obstruct crack propagation which occurs with wear, thus improving WC-Co composite wear resistance. Grain boundaries in nanostructured coatings are more than in ultra-fine coatings and slip is impeded, which hampers crack propagation; the increase in the grain boundary area will improve the mechanical properties of coatings.

As can be seen from Fig. 8(a), there are some drawbacks, including a large number of microscopic cracks and spallation in the worn surface of ultra-fine coating, which indicates that the toughness is low. As for nanostructured coatings, there exists some shallow pits, but no other defects are observed. There is a little original particle coating remaining in worn trace. The layer bonding is weak in ultra-fine coating. With repeating load, the defects and microscopic cracks propagate gradually. Plastic deformation occurred at high temperature during wear. In the plastic deformation process, when the slipping is limited by obstructions (such as grain boundaries, second phase, inclusions, etc.), stress concentration will be created, which may cause cracks of different sizes. The stress concentration will be more serious in ultra-fine coating because of fewer grain boundaries. As a result, ultra-fine coating has low toughness. So it is more likely to create brittle fracture, which will result in production of abrasive particles and the pits formed after shedding of surface coating. We also see the trace of adhesive wear in Fig. 8. The analysis is that brittle fracture, abrasive wear followed with adhesive wear dominates in ultra-fine coating. In nanostructured coating, nano-particles and sub-micron-scale particles exist. The smaller the average grain diameter, the nearer the dislocation source is to the grain boundaries, the fewer are the number of dislocations and the less serious is the stress concentration. In addition, when the average grain diameter is similar to the stress radius, it will make the strain smaller, deformation more homogeneous and less cracks due to stress concentration. So the finer the grain, the better is the plastic deformation. When harmful segregation exists in grain boundaries or brittle phase precipitates, the effect of grain boundaries in obstructing crack propagation is reduced (Ref 13). Therefore toughness is significantly improved. The energy for crack propagating is partly absorbed, thus delaying the crack propagation rate. The nanostructured coating worn surface shows dips shape, which is due to the particles shedding from mating materials and particles shedding from coating in the wearing process. It is considered that fracture and adhesive wear followed with abrasive wear dominate in nanostructured coating.

From Fig. 9, we can observe that the shape and composition of the bright spots in worn surfaces of both the coatings are different. The bright spot of ultra-fine coating shows regular

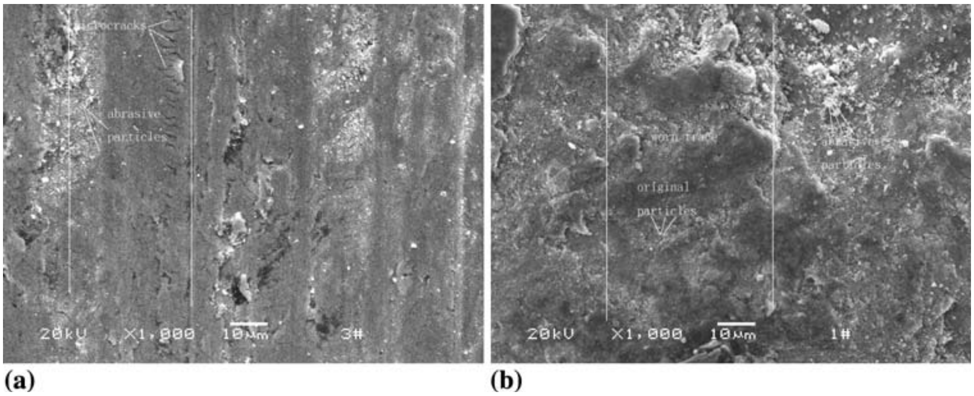

Fig. 8 SEM images of wear surface: (a) worn trace of ultra-fine coating and (b) worn trace of nanostructured coating

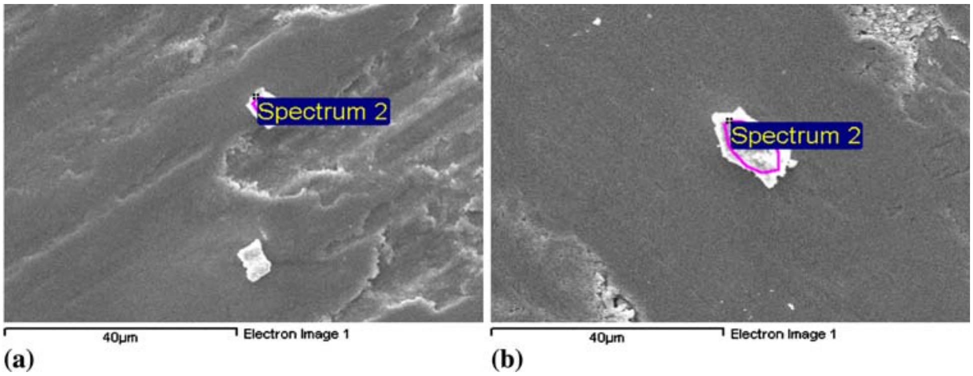

Fig. 9 SEM images of bright particles: (a) bright particles of ultra-fine coatings and (b) bright particles of nanostructured coatings

Table 3 Results of wear surface map scanning

Coating type	C	O	Fe	Co	W
Atomic percentage of ultrafine coating	8.21	50.95	37.86	1.90	1.08
Atomic percentage of nanostructured coating	4.02	57.02	33.12	1.93	3.91

quadrilateral, the EDS analysis of the spots gives oxides of Fe, which is the material transferring from the mating material. The bright spot of nanostructured coating shows hexagon, the EDS analysis of that is a compound of W. The wear test was carried out at elevated temperature. Grain boundary is weaker than grain at high temperature. So besides grain slipping, the adjacent grains will slide along the grain boundaries, which will also cause macroplastic deformation. The plastic deformation is more in nanostructured coating because of more grains per unit volume. So the bright particle is a compound of W in nanostructured coating. And the particle in ultra-fine coating is from the mating material. That is, the performance of ultra-fine coatings in abrasive wear is higher than that of nanostructured coatings.

From Table 3, the results of wear surface map scanning, it is concluded that the content of W is more and the C content is less in nanostructured coating. We considered that compounds of W may exist in the form of W_2C in nanostructured coating, whose content of W_2C is higher than ultra-fine coating. This is consistent with the results of XRD. This can be attributed to the high temperature of flame, fine grain, high area-to-volume ratio, and more complete meting which yields more severe decarbonization. The amount of Fe is lower in ultra-fine coating. Fe is mainly from the mating material by adhesive wear. The degree of adhesive wear of nanostructured coating is less severe. The content of O is more in the nanostructured coating, which indicates more severe oxidation. Some thickness of tribofilm will make contact surface smoother. Thus friction coefficient and the degree of adhesive wear decrease. But if too much tribofilm formed, abrasion will deteriorate wear behavior.

5. Conclusions

(1) The wear resistance of nanostructured coating is better than that of ultra-fine coating under high temperature abrasion test conditions.

(2) The wear mechanism is different between ultra-fine coating and nanostructured coating. Brittle fracture and adhesive wear dominate in ultra-fine coating followed with abrasive wear. Fracture and abrasive wear dominate in nanostructured coating followed with adhesive wear.

(3) The adhesive wear resistance of nanostructured coating is better than that of ultra-fine coating.

Acknowledgment

The authors are grateful to the scientific and technological project Foundation of Chengdu Science & Technology (Grant No. 07GGYB579GX-010).

References

1. F. Zhang, J. Shen, and J. Sun, Processing and Properties of Carbon Nanotubes-Nano-WC-Co Composites, *Mater. Sci. Eng. A*, 2004, **381**(1–2), p 86–91 (in English)
2. B.H. Kear and L.E. McCandlish, Chemical Processing and Properties of Nanostructured WC-Co Materials, *Nanostruct. Mater.*, 1993, **3**(1–6), p 19–30 (in English)
3. B.K. Kim, G.H. Ha, G.G. Lee, and D.W. Lee, Structure and Properties of Nanophase WC/Co/VC/TaC Hard-Metal, *Nanostruct. Mater.*, 1997, **9**(1–8), p 233–236 (in English)
4. H. Zhao, L. Zhu, and X. Ma, New Techniques of Preparing Nanostructured Tungsten Carbides, *J. Mater. Sci. Eng.*, 2003, **21**(1), p 130–134 (in Chinese)
5. P.H. Shipway and D.G. McCartney, Sliding Wear Behavior of Conventional and Nanostructured HVOF sprayed WC-Co Coatings, *Wear*, 2005, **259**(7–12), p 820–822 (in English)
6. B.L. Zha, H.G. Wang, and X.J. Su, Nanostructured WC-12Co Coatings Sprayed by HVO/AF, *Thermal Spray 2004: Advances in Technology and Application*, Verlag fur Schweissen und verwandte Verfahren DVS-Verlag GmbH, Dusseldorf, German, 2004, p 907-909 (in English)
7. Y.Q. Zhang, Z.X. Ding, and Y. Fan, Research on Properties of HVOF Spraying Nanostructured WC-12Co Coating, *Surf. Eng. China*, 2005, **18**(6), p 25–29 (in Chinese)
8. M.F. Morks, M.A. Shoeib, and A.L. Brahim, Comparative Study of Nanostructured and Conventional WC-Co Coatings, *Thermal Spray 2004: Advances in Technology and Application*, Verlag fur Schweissen und verwandte Verfahren DVS-Verlag GmbH, Dusseldorf, German, 2004, p 731-734 (in English)
9. T. Guo, X. Zhou, and W. Lin, et al., The Status and Prospect of Nano-Thermal Spraying Technology, *Surf. Technol.*, 2003, **32**(4), p 1–3 (in Chinese)
10. Q. Yang, T. Senda, and A. Hirose, Sliding Wear Behavior of WC-12%Co Coatings at Elevated Temperature, *Surf. Coat. Tech.*, 2006, **200**, p 4208–4212 (in English)
11. Q. Yang, T. Senda, and A. Ohmori, Effect of Carbide Grain Size on Microstructure and Sliding Wear Behavior of HVOF-Sprayed WC-12%Co Coatings, *Wear*, 2003, **254**, p 23–34 (in English)
12. X.-Q. Zhao, H.-D. Zhou, and J.-M. Chen, Comparative Study of the Friction and Wear Behavior of Plasma Sprayed Conventional and Nanostructured WC-12%Co Coatings on Stainless Steel, *Mater. Sci. Eng. A*, 2006, **431**, p 290–297 (in English)
13. P. Zhao, F. Xie, and Z. Sun, et al., *Materials Science Essentials*, Harbin Institute of Technology Press, Harbin, 2003 (in Chinese)